

Search for point sources of ultrahigh energy γ rays in the southern sky

W.H. Allen,¹ I.A. Bond,² E. Budding,¹ M.J. Conway,² A. Daniel,² K.B. Fenton,³ H. Fujii,⁴ Z. Fujii,⁵
 N. Hayashida,⁶ K. Hibino,⁶ M. Honda,⁶ J.E. Humble,³ S. Kabe,⁴ K. Kasahara,⁷ T. Kifune,⁶
 G.D. Lythe,² A. Masaike,⁸ Y. Matsubara,⁵ K. Mitsui,⁶ Y. Miura,⁴ M. Mori,⁴ Y. Muraki,⁵ M. Nagano,⁶
 T. Nakamura,⁸ M. Nishizawa,⁹ P.M. Morris,² S. Ogio,¹⁰ To. Saito,⁶ M. Sakata,⁹ H. Sato,⁸
 H.M. Shimizu,⁸ M. Spencer,² J.R. Storey,² T. Tanimori,¹⁰ M. Teshima,⁶ S. Torii,⁷
 A. Wadsworth,¹ Y. Watase,⁴ M.D. Woodhams,² Y. Yamamoto,⁹ P.C.M. Yock,² and T. Yuda⁶

(JANZOS Collaboration)

¹*Carter National Observatory of New Zealand, Wellington, New Zealand*

²*Department of Physics, University of Auckland, Auckland, New Zealand*

³*Department of Physics, University of Tasmania, Hobart 7001, Australia*

⁴*National Laboratory for High Energy Physics (KEK), Tsukuba 305, Japan*

⁵*Cosmic Ray Section, STE Laboratory, Nagoya University, Nagoya 464, Japan*

⁶*Institute for Cosmic Ray Research, University of Tokyo, Tokyo 188, Japan*

⁷*Faculty of Engineering, Kanagawa University, Yokohama 221, Japan*

⁸*Department of Physics, Kyoto University, Kyoto 606, Japan*

⁹*Department of Physics, Konan University, Kobe 658, Japan*

¹⁰*Department of Physics, Tokyo Institute of Technology, Tokyo 152, Japan*

(Received 28 December 1992)

A search for point sources of γ rays with energies $\gtrsim 100$ TeV which has been made by the JANZOS Collaboration using an array of plastic scintillators located at Black Birch mountain in New Zealand is reported. The physical characteristics of the array are described, and also the techniques which have been used to analyze the data. Measurements of the angular resolution of the array using the Moon and/or Sun shadowing technique, and also a comparison test with the JANZOS array of Čerenkov mirrors, are reported. About 80 million events were observed in the period October 1987 to January 1992. Upper limits on the average γ -ray fluxes at energies $\gtrsim 100$ TeV from SN 1987A, Vela Pulsar, Vela X-1, LMC X-4, Sco X-1, Cen X-3, SMC X-1, Galactic Center, Cen A, 4U1145-619, 2A1822-371, and PSR1706-44 in this period are reported. The limits are compared with previous measurements which were made at various energies by several groups. Monthly measurements for the flux from SN1987A are also reported, and a search of the southern sky for unknown sources of ultrahigh energy γ rays is described. Some plans for future observations are given.

PACS number(s): 95.85.Pw, 96.40.Pq, 98.70.Dk, 98.70.Qy

I. INTRODUCTION

The JANZOS (Japan Australia New-Zealand Observation of Supernova 1987A) facility was constructed at Black Birch in the South Island of New Zealand (173.78°E, 41.75°S, 1635 m above sea level) to observe ultrahigh energy (UHE) and very high energy (VHE) γ rays emitted by the supernova 1987A in the Large Magellanic Cloud (LMC). It consists of an array of plastic scintillators designed for the observation of air showers produced by cosmic rays and γ rays of energy $\gtrsim 100$ TeV, and an array of Čerenkov mirrors for observations of showers produced by cosmic rays and γ rays with energies $\gtrsim 1$ TeV. The prime motivation for the experiment was the theoretical prediction [1] that, if a neutron star is created in a supernova, and if the neutron star is an efficient accelerator of high energy particles, then UHE and VHE γ rays will be produced copiously in the interaction of high energy particles with the ejecta of the supernova in

the early stage of its development. The JANZOS experiment was planned soon after the discovery of SN 1987A (23 February 1987) and observations commenced on 13 October 1987. The scintillator arrays ran for 1229.16 out of 1568 calendar days (duty cycle 78.4%) in the period October 1987 to January 1992. About 80 million air shower events were accumulated in that time.

The activity of the neutron star in SN 1987A has not been confirmed yet from observations of lower energy photons [2,3] or in the UHE regime [4-8]. In our observations with the JANZOS Čerenkov mirror array [6], a possible signal at the limit of detectability was observed in the \sim TeV region in coincidence with the x-ray "flare" detected by the Ginga satellite on 14-15 January 1988. This TeV γ -ray flare was interpreted as being due to charged particles being accelerated up to a few tens of TeV in the shock wave caused by a collision of supernova ejecta with circumstellar matter, and creating TeV γ rays [9]. If a similar mechanism is effective for 100 TeV

γ rays, the acceleration time is expected to be 1–3 years and emission is expected to continue for a similar period [9]. In this paper we report a search of our UHE database for evidence of such emission from SN 1987A, as well as for emission from the neutron star as described in Ref. [1].

Some technical features of the JANZOS facility are also reported in this paper. The angular resolution of the array has been experimentally measured, by comparison tests with the mirror array, and by the shadowing effect of the Sun and the Moon on cosmic rays, and found to be $\sim 1.25^\circ$ or better. Also, the electron size spectrum recorded by the array has been compared with spectra obtained by other groups. Spectral measurements are sparse in the region covered by the JANZOS array (100–3000 TeV) and we compared our spectrum with the extrapolations of spectra previously obtained at higher energies [10], and at lower energies [11,12]. It is, of course, important to check that there are no systematic biases in the observations. We have also studied the uniformity of the arrival direction of cosmic rays by the method of harmonics analysis, and found that our data set is quite uniform. In this analysis, the concept of “good day” and “good-day data” are introduced to reduce systematic effects from human interference.

Some effort was made to attempt to ensure continuous and stable operation of the array since observations were commenced in October 1987. This has enabled long duration observations to be made of SN 1987A, and other possible sources of UHE radiation in the southern sky. The range of declinations covered is from $\delta = -10^\circ$ to $\delta = -75^\circ$. Stable operation is of course important for the observation of time-dependent phenomena (bursts, periodic emission, etc.).

We note here that previous studies of UHE emission have been made for several southern objects. Clay *et al.* [13] reported emission by Cen A at energies $\sim 10^{15}$ eV from 1979 to 1981 and from 1984 to 1987. Protheroe *et al.* [14] reported periodic emission by Vela X-1 and by

LMC X-4 at energies $\sim 10^{16}$ eV during 1979 – 1981. Meyhandan *et al.* [15] subsequently reported periodic emission by LMC X-4 at energies $\sim 10^{17}$ eV. Ciampa *et al.* [16] reported periodic emission from the x-ray binary 2A1822-371 at energies $\sim 10^{15}$ eV, and Clay *et al.* [17] subsequently reported periodic emission from this object at energies $\sim 10^{17}$ eV. Finally, Tonwar *et al.* [18] reported a burst of emission by Sco X-1 at energies $\sim 10^{14}$ eV. This observation was subsequently confirmed by Meyhandan *et al.* [19]. The periodic emissions reported above were all at the orbital periods of the various x-ray binary systems.

II. THE JANZOS SCINTILLATOR ARRAY

The JANZOS detector for the UHE region is an array of plastic scintillators designed for the observation of air showers produced by cosmic rays and γ rays with energies $\gtrsim 100$ TeV. It consists of 45 0.5-m^2 scintillators and 31 1-m^2 scintillators. A sketch of the detectors and their positions is given in Fig. 1. The 0.5-m^2 detectors are shown by downward triangles and the 1-m^2 detectors by upward triangles. The positions of the three Čerenkov mirrors of the JANZOS VHE detector are also shown in the same figure by circles. The south direction represented in Fig. 1 is parallel to the grid system of the New Zealand Department of Land Survey. The true south direction is 1.51° west from the grid south at the JANZOS site. We determined the position of the observation site, and the true south direction, by observations of several bright stars. The observed positions agreed with the expected positions to within 0.05° .

The 0.5-m^2 scintillators are viewed by fast rise-time 2-in. photomultipliers (Hamamatsu Photonics H1949) for the purpose of carrying out timing and particle density measurements in air showers. The timing measurements are used to determine arrival directions of air showers. For each 1-m^2 detector, a relatively slow 5-in. photomul-

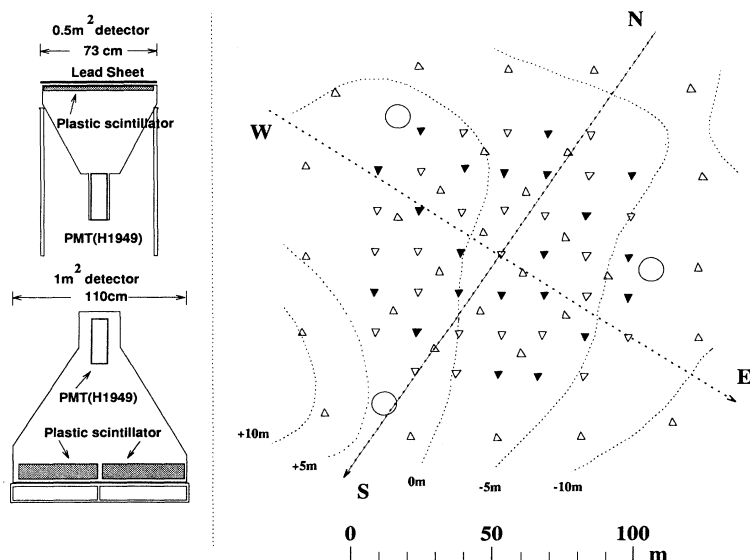


FIG. 1. The JANZOS scintillator detectors and layout of the facility. Downward solid triangles represent the positions of odd numbered 0.5-m^2 detectors, downward open triangles the positions of even numbered 0.5-m^2 detectors, and upward ones the positions of 1-m^2 detectors. The open circles show the positions of 2-m diameter Čerenkov mirrors.

plier (Hamamatsu Photonics R877) and an amplifier was installed initially to measure particle densities only. In order to increase the dynamic range of the density measurements, the amplifiers were subsequently removed and the 5-in. photomultipliers replaced by 2-in. ones, of the same type used with the 0.5-m² detectors. This improvement was made in January 1989.

A lead sheet with a thickness of one radiation length was placed on top of each 0.5-m² detector. The lead converts γ rays in air showers to electrons and positrons by pair creation and/or Compton scattering, and renders the detectors sensitive to low energy γ rays in air showers [20]. There is a large number of soft γ rays in an electromagnetic cascade, and the lead sheets effectively enlarge the detector area by a factor of ~ 2 . The effect of the lead is included in the air shower analysis of the data.

A block diagram of the electronics for the array is shown in Fig. 2. The output of each 0.5-m² detector is divided into three, and led to a triggering unit, a time-to-digital converter (TDC, Kaizu 3780), and an analogue-to-digital converter (ADC, LeCroy 2249W). The outputs of the 16 outer 1-m² detectors are divided into two, and led to TDC's and ADC's, while the outputs of the 15 inner 1-m² detectors are led to ADC's only. The TDC's and ADC's are connected to a CAMAC dataway which is controlled by a 16-bit personal computer (PC-9801VX, NEC). When three or more 0.5-m² scintillators produce pulses higher than the 1.5-particle level within 100 ns, the triggering unit generates a trigger pulse for the recording system. For each triggered event, the timing and pulse height data from each detector are stored on 8-mm videotape, together with the overall time of the event as given by an atomic clock.

The operation of the array is quite well automated. Automatic operation is possible for periods of about one month. A modem monitoring system, using a telephone line, was installed to monitor the running conditions of the telescope, and to signal power failures, etc.

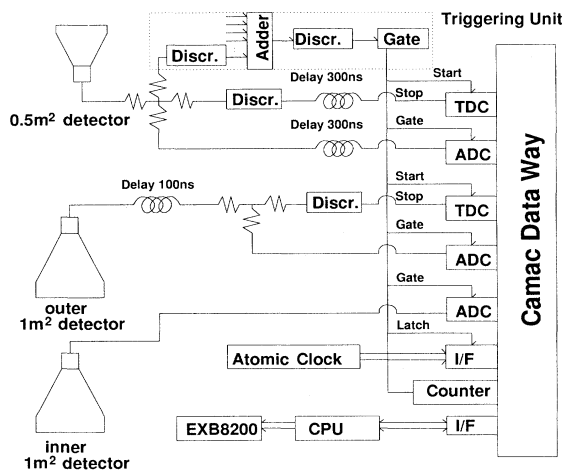


FIG. 2. The electronics block diagram of the JANZOS scintillator array.

III. CALIBRATION OF THE SCINTILLATOR ARRAY

The timing measurement system of the scintillator detector is calibrated at regular intervals with a TDC checker and by using cosmic-ray muons. A block diagram of the muon calibration system is shown in Fig. 3. The reference scintillation detector is used to detect muons and to trigger the recording system. Similar measurements are made for all the timing detectors using the same reference detector and cable. The relative TDC values obtained in these measurements give the relative delays of each detector, including the differences of the photomultiplier transit times, of the cable lengths, of the time delays in the discriminators, and of the offsets of the time-to-digital converters. A common delay has no effect on the determination of arrival directions of cosmic rays. The TDC checker is used to determine the conversion factors of the time-to-digital converters.

The relative delay times of the detectors are also measured with a laser system. Coincident signals from a pulsed N₂ laser are led to each photomultiplier via a system of optical fibers of equal length. The TDC values recorded by the detectors provide an independent measure of the relative delay times.

We measure a "shower thickness parameter" $C_{\text{thickness}}$ for the correction of timing data in the muon calibration runs. The correction formula we use is

$$T_{\text{corr}} = T_{\text{raw}} - C_{\text{thickness}} \frac{1}{\sqrt{n}}. \quad (3.1)$$

Here T_{raw} denotes the raw timing data in ns, T_{corr} the corrected timing data, and n the particle number recorded by a detector. Equation (3.1) reflects the fact that a detector near the core of a shower records the passage of the shower front, whereas those on the perimeter of a shower record, on average, the passage of the shower mid-plane. This equation includes the effect of "time walk" which occurs in the photomultipliers and the discriminators. The muon calibration runs described above include clearly identifiable air shower events, as well as single muon events. The former are used to measure the thickness parameter $C_{\text{thickness}}$. We find $C_{\text{thickness}} \sim 8$ ns, which is a little larger than the value obtained by Gaisser

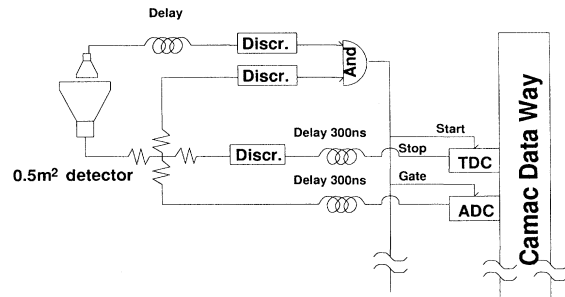


FIG. 3. The triggering unit used for muon calibrations. The other parts of the electronics are as for normal operation (Fig. 2).

et al. [21] because it includes the effect of time walk.

Small drifts in the timing electronics of order 1 ns per year per channel occur. These may be observed by comparison of data obtained in successive muon and laser calibration runs. These drifts are corrected for in off-line analysis of the data. From the timing data we can calculate the time when any shower passes the coordinate origin of the scintillator array. Knowing this time, and the arrival direction of the shower, the times when the shower passes each detector can be calculated. If a drift occurs in a particular channel, this can be identified as a systematic displacement of the calculated passage times for that channel away from the observed times for a sample of events. In this way we allowed for small drifts which occurred in the timing electronics between successive muon or laser calibrations.

The gains of the photomultipliers were examined by the ADC spectra of the detectors. At the experimental site, ADC spectra were accumulated for small samples of air shower events and the single particle peaks were used to set the high voltages of the photomultipliers. In subsequent off-line analysis, these spectra were studied in more detail using samples of one or more days of air shower events. We found that the single particle levels determined in air shower events were quite consistent with those obtained in muon calibration runs.

IV. RECONSTRUCTION OF CORE POSITIONS, ARRIVAL DIRECTIONS, AND ELECTRON SIZES OF AIR SHOWERS

Arrival directions of air showers were determined by a least-squares method. If we define l, m, n as the direction cosines of a shower, t_i as the time when the shower front passes detector i , and x_i, y_i, z_i as the coordinates of detector i , then we have

$$lx_i + my_i + nz_i = -c(t_i - t_0), \quad (4.1)$$

where c is the velocity of light and t_0 is the time when the shower front passes the coordinate origin. The shower front is assumed at this stage of the analysis to be a plane, perpendicular to the arrival direction of the primary cosmic ray. In the least-squares method, the parameters l, m, n , and t_0 are varied, subject to the restriction that $l^2 + m^2 + n^2 = 1$, so that

$$\chi^2 = \sum_i W_i [lx_i + my_i + nz_i + c(t_i - t_0)]^2 \quad (4.2)$$

is minimized. Here W_i is the statistical weight of the measured time t_i . We assumed

$$W_i \propto n_i^\alpha, \quad (4.3)$$

where n_i is the number of particles recorded by detector i . We found with $\alpha \sim 2$ that the statistical weights were self-consistent, i.e., $W_i = \sigma_i^{-2}$ where σ_i is the standard deviation of the i th time measurement.

The core positions and the electron numbers (N_e) of showers were determined by fitting the observed particle

densities to the NKG (Nishimura-Kamata-Greisen) function with a variable age parameter.

It has been pointed out by many authors that when the angular resolution of the arrival direction measurements approach one degree, a correction to the plane geometry for the shower front is necessary [22]. In our study, we have found, however, that only a small correction is necessary when we employ the shower thickness correction to the timing data as explained above [Eq. (3.1)]. Assuming a conical shape to the shower front, i.e.,

$$T'_{\text{corr}} = T_{\text{corr}} - \beta r, \quad (4.4)$$

where r is the perpendicular distance of a detector from the shower core, we found (see below) $\beta \sim 0.035$ ns/m. This value of the cone angle is consistent with that determined by Gaisser *et al.* (Ref. [21]). Its smallness implies that the accuracy with which the position of the core of a shower is determined is not crucial. Statistical fluctuations in the timing measurements, which result from the finite thicknesses of air showers, control the precision with which arrival directions may be determined.

The angular resolution of the arrival direction measurements may be effectively improved by data selection techniques. We divided the array into two overlapping arrays of even-numbered and odd-numbered detectors, as shown in Fig. 1, and determined the arrival direction of each shower twice, using the two independent arrays. In our studies of point sources of UHE γ rays, we selected only those events for which the arrival directions agreed to better than 5° . We further discarded events with cores lying outside the array ($R_{\text{core}} > 60$ m). Approximately one third of all events survived these selections. A Monte Carlo simulation of this sample of events indicated that their arrival directions were determined within an error of 1.25° in 50% of the events.

We also examined the angular resolution of the scintillator array by comparing measured arrival directions of showers near the zenith which were detected by both the scintillator and mirror arrays. The mirror array was used to observe the supernova at small zenith angles for three seasons: Nov. 1987 – Jan. 1988, Nov. 1988 – Feb. 1989, and Nov. 1989 – Feb. 1990. For this test we used the data of Nov. 1989 – Feb. 1990. The typical energies of cosmic rays which are observed by the scintillator array (~ 100 TeV) and the mirror array (~ 3 TeV) differ greatly, and the rate at which both arrays observe common events is small. After the event selections described above, there were 1240 events which remained. This was sufficient for a measurement of the angular resolution to be made. The distribution of differences of arrival directions determined by the two systems is shown in Fig. 4. Since the average zenith angle of SN 1987A for these observations was $\sim 30^\circ$, the azimuth difference shown in the figure is twice the true angular difference ($\text{csc}30^\circ$). We found that 627 events, which is a little more than 50% of the common events, lie within the circle of radius of 1.25° . The accuracy of arrival directions determination by the JANZOS mirror array is $\sim 0.7^\circ$ (see Ref. [23]), and from this we deduce that the angular resolution of JANZOS scintillator array is somewhat better than 1.25° . In

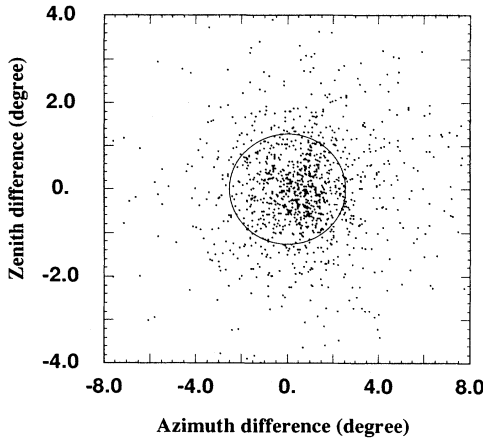


FIG. 4. The difference of arrival directions determined by the scintillator and mirror arrays. The average zenith angle is $\sim 30^\circ$, and therefore the true angle difference in the azimuth direction is half the azimuth difference.

the course of carrying out this comparison we tried various values for the cone angle for the correction for the shower front [Eq. (4.4)], and found that 0.035 ns/m gave the best result when the shower thickness correction of the timing data was included. Without this correction, a cone angle of 0.125 ns/m gave the best result.

We also studied the shadowing effect of the Moon and the Sun on cosmic rays. In our data sample used for this test, there were 32 299 air showers within a cone of 5° around the Sun and the Moon for which zenith angle was less than 30° . Figure 5 shows the combined effect of shadowing by the Sun and the Moon plotted against the angular distance from their centers. The shadowing effect is seen in this figure, and it is consistent with our expectation from a Monte Carlo simulation assuming an angular resolution of 1.25° . The angular resolution may be better than 1.25° . It is, however, difficult to determine precisely from the shape of the shadow, because of the low statistics involved.

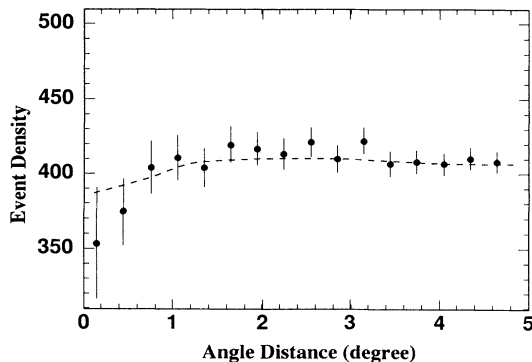


FIG. 5. Event density vs angular distance from the center of the Sun and the Moon. The dashed line represents an expectation from a Monte Carlo simulation assuming an angular resolution of 1.25° for the scintillator array.

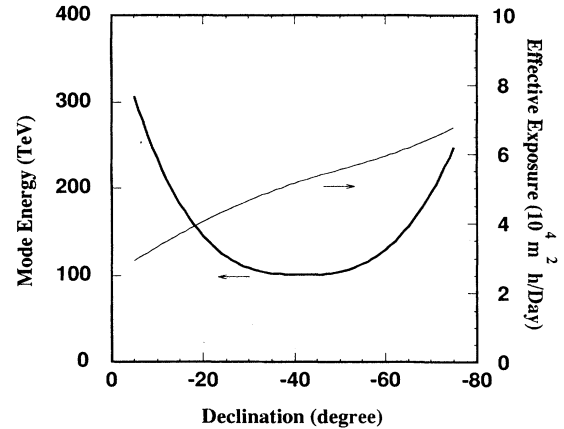


FIG. 6. E_{mod} and effective exposure dependence on declination. The thick solid line represents E_{mod} for source spectra proportional to $E^{-2.0}$.

Finally, we studied the threshold energy and effective area of the scintillator array by a Monte Carlo simulation [24]. The threshold energy for γ rays, and the effective area, vary with the zenith angle, and, therefore, with declination. We express the typical energy of γ rays observed by the array as the *mode* energy (E_{mod}) which we define as the energy which maximizes $dN(\geq E)/dE$. We determined the effective area from the one-day exposure above E_{mod} . Assuming an energy spectrum for UHE γ -rays sources proportional to $E^{-2.0}$, the results are as shown in Fig. 6.

V. CHARACTERISTICS OF COSMIC RAYS MEASURED WITH THE SCINTILLATOR ARRAY

The size spectrum of air showers was studied to confirm the energy region we are observing and as a preliminary study of the energy spectrum. We used showers which satisfied $\cos(\theta_{\text{zenith}}) > 0.9$ and for which the core position was inside a $70 \text{ m} \times 70 \text{ m}$ area centered on the array. The core distribution is uniform over this area. Arrival directions need not be known precisely in the determination of the energy spectrum and, in order to extend the measurements to lower energies, we analyzed events for which the even and odd subarrays gave consistent arrival directions to within 20° . The results are as shown in Fig. 7.

The solid line in Fig. 7 shows the expected electron size spectrum as calculated from the primary cosmic-ray spectrum for $E < 4700 \text{ TeV}$ given with $w = 1.4$ in Ref. [10]:

$$J(E)dE = 0.165(\text{m}^{-2} \text{ s}^{-1} \text{ sr}^{-1} \text{ TeV}^{-1}) \times \left(\frac{E}{1 \text{ TeV}} \right)^{-2.62} dE \quad (5.1)$$

and from the relation between electron size and primary energy in our experiment:

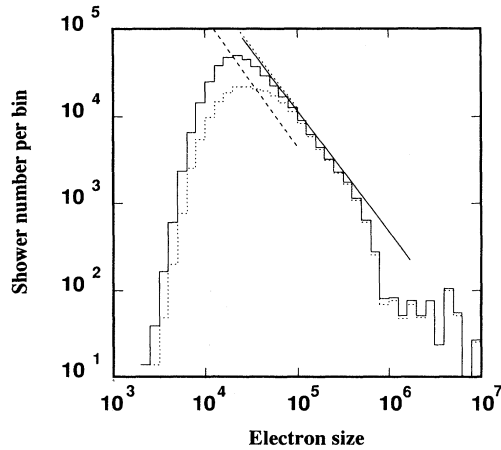


FIG. 7. Electron number spectrum of showers observed in the JANZOS experiment. The solid line histogram shows the spectrum for all analyzed data and the dotted one is for those events for which the difference of the arrival directions determined by the even and odd subarrays was less than 5° . The solid straight line represents the expected electron number spectrum from the cosmic-ray energy spectrum in the upper energy region [10]. The dotted line is the expected spectrum in the lower energy region using data from Ref. [11] and dashed line from Ref. [12].

$$E = 2.1 \times 10^{-2} N_e^{0.86} (\text{TeV}). \quad (5.2)$$

Equation (5.2) was obtained by a Monte Carlo simulation. In the equation N_e denotes the electron number at the altitude of the array. This is determined from the pulse heights recorded by the detectors, after correcting (Amenomori *et al.*, Ref. [22]) for the effect of the lead sheets on them. We compared Eq. (5.2) with the equivalent relation used by the Akeno group (Ref. [10]), and found that it was closely consistent when the difference in altitude of the two arrays is taken into account. The dotted and dashed lines were calculated by the same method but using extrapolations of lower energy cosmic ray spectra [11,12]. The observed electron size spectrum agrees with the expected ones calculated from other experiments to the level that the other experiments agree, in the region $100 \sim 3000$ TeV.

The breakdown of the spectrum in Fig. 7 at $N_e \sim 6 \times 10^5$ is due to saturation of the ADC's employed in the experiment and it does not represent a physical effect. For these showers we cannot determine the core position or N_e well by fitting to the NKG function. However, we can determine the arrival direction rather accurately, since our determination of arrival direction depends only weakly on the position of the core of a shower.

In studies of point sources of UHE γ rays, the arrival distribution of all cosmic rays (charged and neutral) is measured. Statistically significant excesses in particular directions are assumed to be caused by point sources of γ rays. The validity of the method is justified if the arrival distribution of charged cosmic rays is quite isotropic, so

that it can be represented by a smooth function except for statistical variations.

To study the arrival distribution of cosmic rays as a function of right ascension, we took 6 declination bands: $\delta > -12^\circ$, $-12^\circ > \delta > 27^\circ$, $-27^\circ > \delta > -42^\circ$, $-42^\circ > \delta > -57^\circ$, $-57^\circ > \delta > -72^\circ$, and $-72^\circ > \delta$. We selected showers with $R_{\text{core}} < 60$ m and for which the even and odd subarrays gave consistent directions to within 20° . The distributions of arrival directions so obtained are shown in Fig. 8. The analysis was made by the method of harmonics analysis. The curves are the fitted results up to the second harmonic. The amplitudes are $\lesssim 5 \times 10^{-3}$ for the first harmonic and $\lesssim 2.5 \times 10^{-3}$ for the second harmonic for all declination bands. We note that in the declination bands of $-27^\circ > \delta > -42^\circ$ and $-42^\circ > \delta > -57^\circ$, the amplitudes are very small. If we combine the two bands, the amplitudes are 2.39×10^{-3} for the first harmonic and 1.99×10^{-3} for the second harmonic. These amplitudes are similar in magnitude to those reported by Linsley (Ref. [25]) and we conclude that the distribution of arrival directions in our data set is quite uniform.

We introduced the concepts of “good days” and “good-day data” to study the distribution of cosmic-ray arrival directions in our database, and to attempt to understand the nature of the variation of the distribution with di-

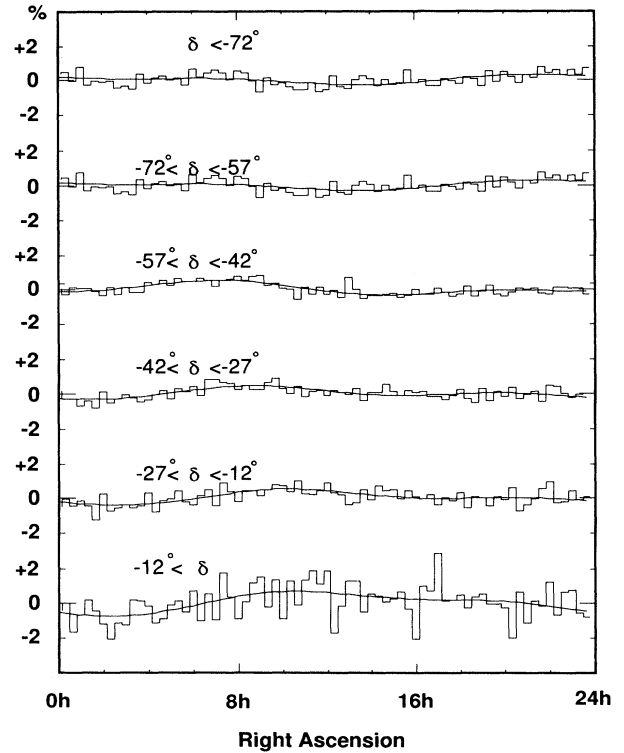


FIG. 8. Arrival direction distribution of cosmic rays from all-day data in the declination bands: $\delta > -12^\circ$, $-12^\circ > \delta > 27^\circ$, $-27^\circ > \delta > -42^\circ$, $-42^\circ > \delta > -57^\circ$, $-57^\circ > \delta > -72^\circ$, and $-72^\circ > \delta$. The best fit curves with Fourier series up to second order are also shown.

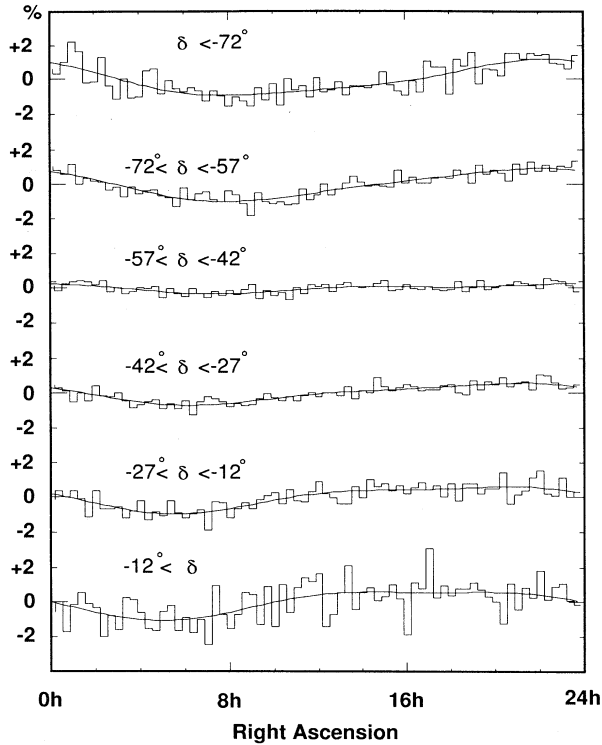


FIG. 9. Arrival direction distribution of cosmic rays from good-day data in the declination bands: $\delta > -12^\circ$, $-12^\circ > \delta > -27^\circ$, $-27^\circ > \delta > -42^\circ$, $-42^\circ > \delta > -57^\circ$, $-57^\circ > \delta > -72^\circ$, and $-72^\circ > \delta$. The best fit curves with Fourier series up to second order are also shown.

rection. When the experiment ran for longer than one sidereal day without any stops longer than 5 min, we divided the running time from the start into complete sidereal days. We refer to these days as “good days” and to data contained therein as “good-day data.” We have 1014 good days in the total operation time (1229.16 days) and $\sim 82\%$ of all events may be retained as good-day data. The distributions of arrival directions with

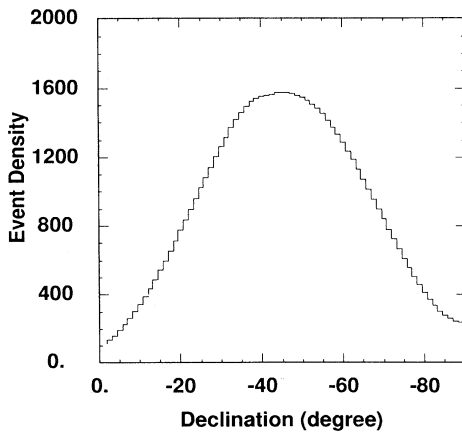


FIG. 10. The variation of the measured arrival distribution with declination averaged over right ascension.

this “good-day data” are shown in Fig. 9. The amplitudes for combined data in the two declination bands of $-27^\circ > \delta > -42^\circ$ and $-42^\circ > \delta > -57^\circ$ are 3.78×10^{-3} for the first harmonic, and 1.34×10^{-3} for the second harmonic, comparable to the values mentioned above. We have not yet corrected the data for the effects of temperature and pressure variations. In the future we plan to incorporate these effects to attempt to measure the anisotropy of the arrival distribution of UHE cosmic rays.

Finally, in Fig. 10 we show the arrival distribution averaged over right ascension as a function of declination. We find that the distribution has a maximum at $\delta \sim -45^\circ$ and that it slopes steeply in both directions. Thus it is difficult to calculate expected event numbers from the event distributions in different declinations.

VI. MEASUREMENT OF UHE γ -RAY FLUXES FROM KNOWN OBJECTS

We studied the UHE γ -ray fluxes from several objects which have previously been reported as UHE γ -ray sources [13–19] and also from various objects which are known to be active in the radio and/or x-ray energy region. We used the method of scanning in right ascension. We took a window around an object with a radius of 1.25° , which is the angular resolution of the array, and compared the number of events from the window with the numbers from others which have the same radius and declination but different right ascensions. This method is free from the large variation of event number density which occurs in the direction of changing declination. The result of right ascension scans for SN 1987A, Vela X-1, and the Galactic Center are shown in Fig. 11 for all-day data and in Fig. 12 for good-day data. Only those showers with cores within 60 m of the center of the array and arrival directions, as determined by the even and odd subarrays, equal to within 5° were included. The curves in Figs. 11 and 12 show the most probable expectation values of event numbers as explained below. We find that these curves are similar to the ones for cosmic-ray arrival directions at similar declinations.

The excess number of events in a source window, and the flux from an object, were calculated using a method similar to the one proposed by Protheroe [26]. In our case, however, the variation of event numbers in the reference windows is small. Consequently it was not necessary to take a limited set of reference windows. We used all windows at a given declination as reference windows using a method of parameter fitting.

In the method of Protheroe, the event numbers in the reference windows, and in the source window without its excess events, are parametrized by a function $N_B(\theta_i : \alpha, \beta, \dots)$. Here θ_i is the right ascension of the center of window i ($i = 0$ for the source window) and α, β, \dots are fitting parameters. Assuming that the event numbers follow a Poissonian distribution, the probability with which the excess number from a source is N_{ex} and the background event numbers in the windows are N_0, N_1, N_2, \dots is proportional to the event number distribution function:

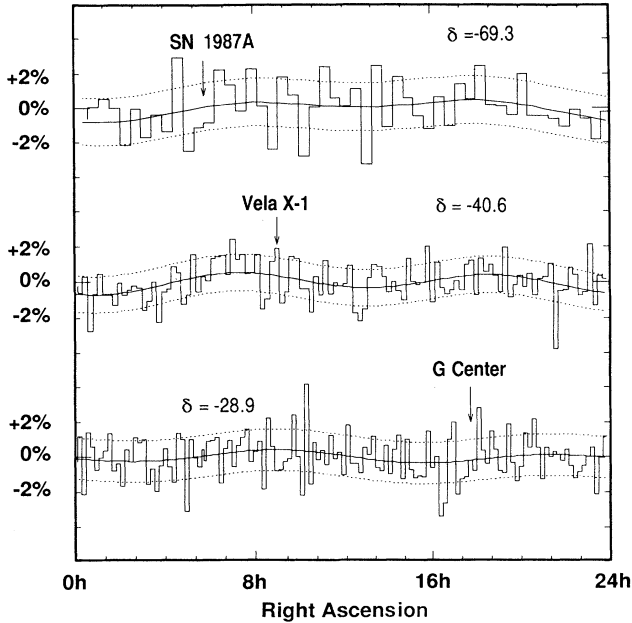


FIG. 11. Right ascension scans for SN 1987A, Vela X-1, and the Galactic Center using all-day data. The solid line shows the expected background number and the dotted lines are one standard deviation limit.

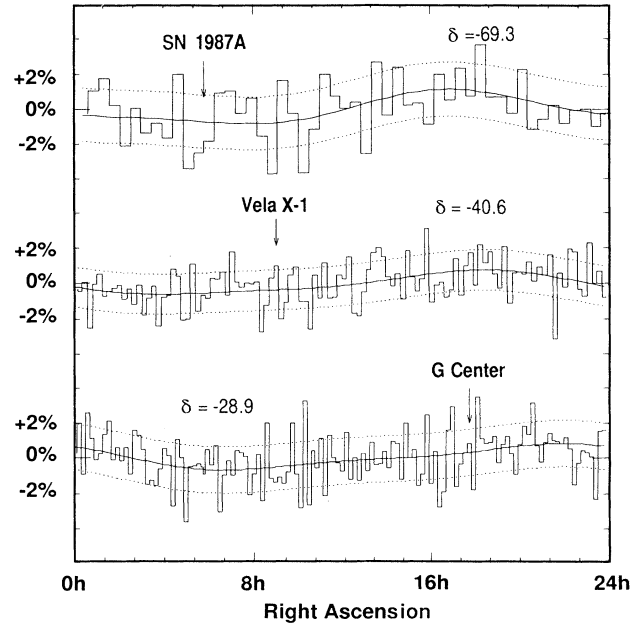


FIG. 12. Right ascension scans for SN 1987A, Vela X-1, and the Galactic Center using good-day data. The solid line shows the expected background number and the dotted lines are one standard deviation limit.

$$D(N_{\text{ex}}, N_0, N_1, N_2, \dots) = \sum_{N'=0}^{N_{\text{ex}}} B(p, N', N_{\text{ex}}) \int \int \dots d\alpha d\beta \dots \left[P(N_0, N' + N_B(\theta_0 : \alpha, \beta, \dots)) \times \prod_{i \neq 0} P(N_i, N_B(\theta_i : \alpha, \beta, \dots)) \right]. \quad (6.1)$$

Here p denotes the probability that a source event has a measured arrival direction falling within the source window, $B(p, M, N)$ is the binomial distribution: $\binom{N}{M} p^M (1-p)^{(N-M)}$, and $P(N, M)$ is the Poissonian distribution: $e^{-M} \times M^N / N!$. The event number distribution is defined as the sum of probabilities of all possible cases. The in-

tegrations of α, β, \dots , are over all the possible parameter ranges. The summation parameter N' denotes the number of source events whose direction is reconstructed in the source window. The probability that the number of excess events from the source is more than N_{ex} is given

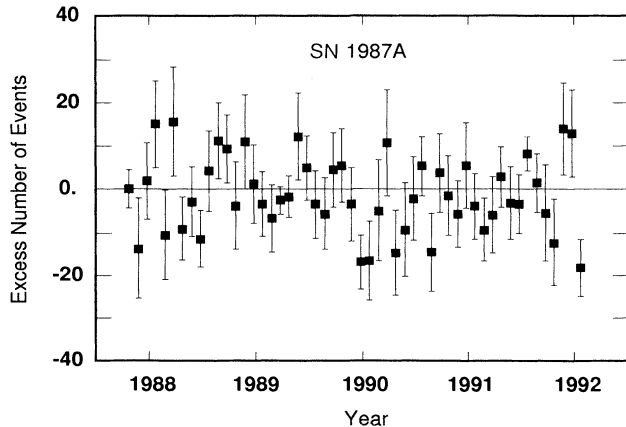


FIG. 13. Monthly variation of the difference *observed-background* in the window of SN 1987A.

TABLE I. The list of upper bound for possible UHE γ -ray sources in the southern hemisphere including the supernova 1987A.

Object	$E_{\text{mod}}(\text{TeV})$	Flux upper bound ($10^{-13} \text{cm}^{-2} \text{s}^{-1}$)	
		All-day data	Good-day data
SN 1987A	190	1.01	0.99
Vela Pulsar	100	2.58	2.56
Vela X-1	100	2.31	2.14
LMC X-4	165	1.59	1.61
Sco X-1	180	2.39	2.59
Cen X-3	130	1.09	1.56
SMC X-1	200	1.36	1.66
Galactic Center	110	1.76	2.18
Cen A	105	3.29	3.24
4U1145-619	130	1.05	1.10
2A1822-371	100	1.68	2.17
PSR1706-44	105	1.49	1.81

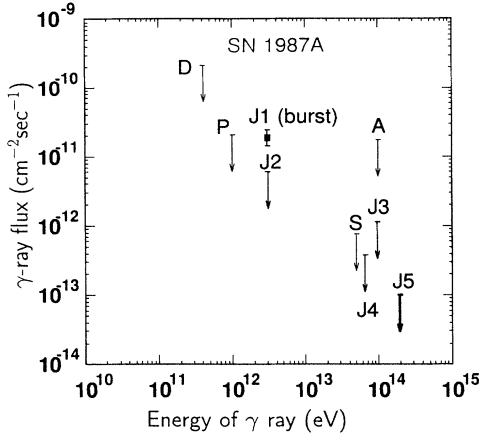


FIG. 14. Comparison of results obtained in various experiments on the flux of high energy γ rays from SN 1987A. *D* is from Ref. [27], *P* from [28], *J1* and *J2* from [5], *S* from [29], *A* from [30], *J3* from [31], *J4* from [32], and *J5* from this paper.

by the relation

$$\text{Prob}(\geq N_{\text{ex}}) = \frac{\sum_{N'_e=N_{\text{ex}}}^{\infty} D(N'_e, N_0, N_1, \dots)}{\sum_{N'_e=0}^{\infty} D(N'_e, N_0, N_1, \dots)}. \quad (6.2)$$

For our analysis we took a function similar to the Fourier series as the fitting function for event numbers:

$$N_B(\theta) = \sum_{i=0}^{N_{\text{max}}} \alpha_i \cos(i \cdot \theta) + \sum_{i=1}^{N_{\text{max}}} \beta_i \sin(i \cdot \theta). \quad (6.3)$$

We normally took $N_{\text{max}} = 2$ since a larger value of N_{max} gave almost the same result but required a longer computation time.

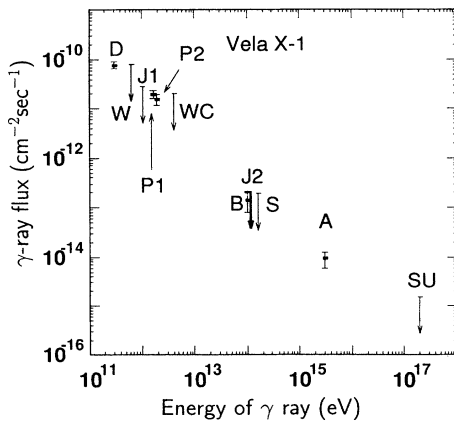


FIG. 15. Comparison of results obtained in various experiments on the flux of high energy γ rays from Vela X-1. *D* is from Ref. [33], *W* from [34], *J1* from [23], *P1* from [35], *P2* from [36], *WC* from [37], *J2* from this paper, *B* from [38], *A* from [14], and *SU* from [15].

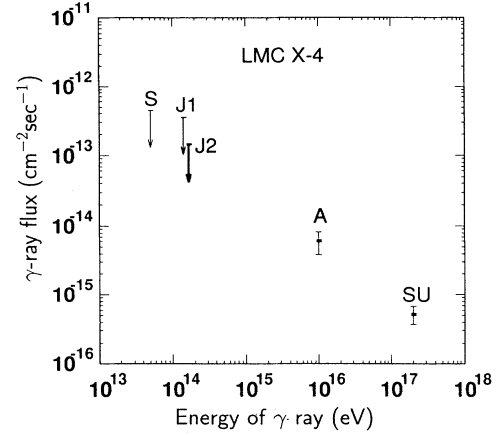


FIG. 16. Comparison of results obtained in various experiments on the flux of high energy γ rays from LMC X-4. The authors of Ref. [15] note that the point at the highest energy may, in fact, apply to particles other than photons. *S* is from Ref. [29], *J1* from [32], *J2* from this paper, *A* from [14], and *SU* from [15].

When there is a positive N_{ex} with a $\text{Prob}(\geq N_{\text{ex}})$ larger than 0.95, it may be concluded that the object being studied is a source of UHE γ rays at the 95% confidence level. If no such large probability for a positive excess number exists, a 95% confidence limit on the excess may be calculated as the value of N_{ex} which satisfies $\text{Prob}(\geq N_{\text{ex}}) = 0.05$. Once an excess number is obtained, it is straightforward to calculate the flux of UHE γ rays from the effective exposure given in the former section and the observation time. An upper bound on a flux may be calculated in the same way.

In Table I, upper bounds obtained in the above manner for various UHE γ -ray source candidates are listed. These are for continuous emission during the period October 1987 to January 1992 and they assume source spectra

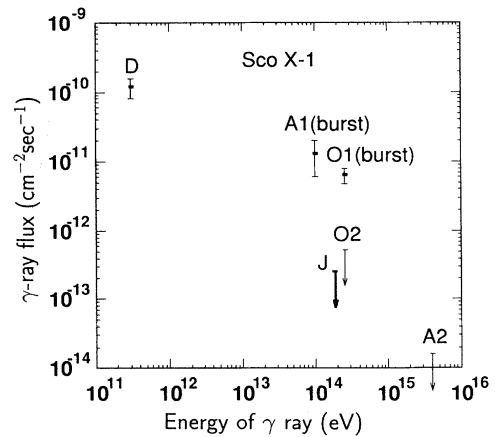


FIG. 17. Comparison of results obtained in various experiments on the flux of high energy γ rays from Sco X-1. *J* is from this paper, *O1* and *O2* from Ref. [18], *A1* from [19], *A2* from [14], and *D* from [39].

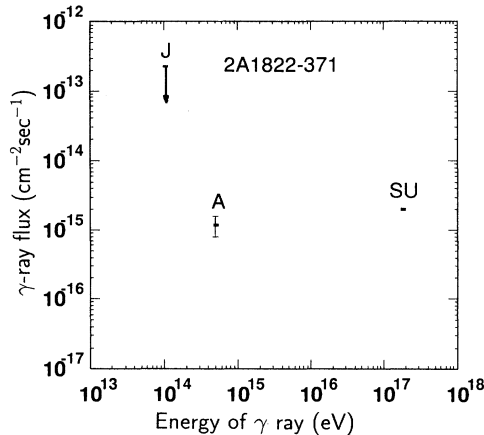


FIG. 18. Comparison of results obtained in various experiments on the flux of high energy γ rays from 2A1822-371. The authors of Ref. [17] note that the point at the highest energy may, in fact, apply to particles other than photons. J is from this paper, A from Ref. [16], and SU from [17].

proportional to E^{-2} . In the calculations for the extra galactic sources (SN 1987A, etc.), the effect of absorption of γ rays by the 2.7-K background radiation was taken into account.

In Fig. 13 we plot the monthly variation of the difference of the observed and expected background event numbers for SN 1987A using good-day data only. These variations are consistent with Poissonian fluctuations.

The results of the present experiment are compared with those from other experiments in Figs. 14–20. The comparison is made for those objects which have been studied by several groups. In general, the results of the various experiments appear to be consistent, except probably in the case of the x-ray binary 2A1822-371. Further observations of this object would be useful.

We note here that the air shower techniques employed in these experiments cannot guarantee that a positive

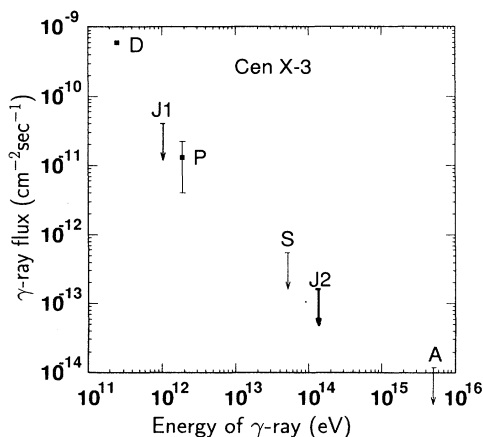


FIG. 19. Comparison of results obtained in various experiments on the flux of high energy γ rays from Cen X-3. D is from Ref. [39], P from [40], S from [29], $J2$ from this paper, A from [14], and $J1$ from [23].

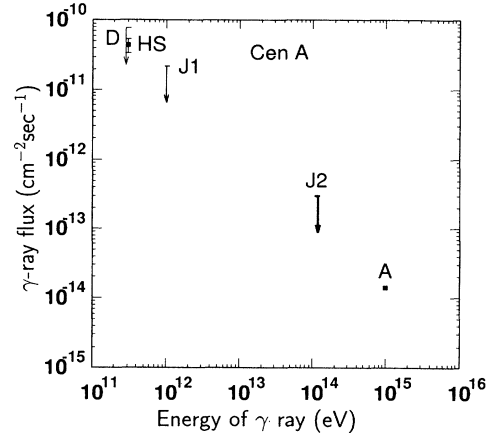


FIG. 20. Comparison of results obtained in various experiments on the flux of high energy γ rays from Cen A. The authors of Ref. [13] note that the point at the highest energy may, in fact, apply to particles other than photons. HS is from Ref. [41], D from [42], $J2$ from this paper, A from [13], and $J1$ from [23].

detection results from an incident flux of photons. The authors of Refs. [13–17] remarked that the positive results reported by them for the objects LMC X-4, 2A1822-371, and Cen A may apply to particles other than photons.

VII. ALL-SKY SEARCH FOR UHE γ -RAY SOURCES

We made a search for unknown UHE γ -ray sources in the southern sky by searching for peaks in the distribution of arrival directions using good-day data. Except for statistical fluctuations, the distribution is a slowly varying function of right ascension. It is, however, a rapidly varying function of declination (see Fig. 10). We made right ascension scans to cover the sky from $-10^\circ \geq \delta \geq -75^\circ$. We used a square window of real size

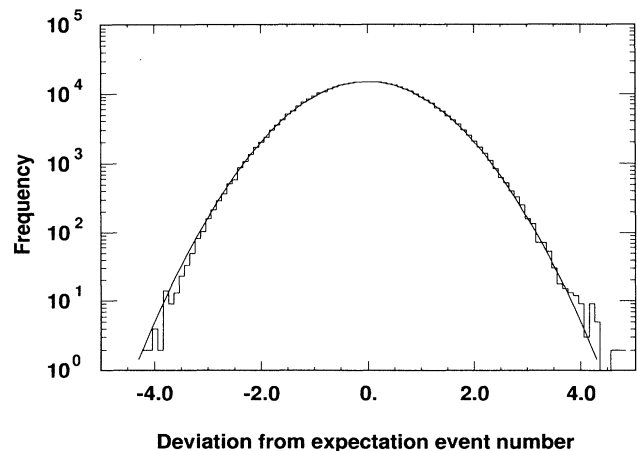


FIG. 21. Deviation spectrum in unit of the standard deviation.

TABLE II. The list of direction in the all-sky search for unknown UHE γ -ray sources with excess counts $> 4\sigma$.

Right ascension	Declination	Excess (σ)
$1^h 1' 30''$	-61.00°	4.72
$13^h 46' 30''$	-17.25°	4.19
$16^h 23' 0''$	-20.25°	4.19
$0^h 52' 30''$	-17.50°	4.12
$21^h 9' 0''$	-22.75°	4.10
$16^h 11' 0''$	-56.75°	4.05
$8^h 10' 0''$	-39.25°	4.05

$2.25^\circ \times 2.25^\circ$ to match the area of a circular window of radius 1.25° . Overlapping windows were used with incremental shifts of 0.25° in declination and right ascension.

The spectrum of deviations that was obtained is shown in Fig. 21 in units of standard deviations (σ) for all right ascension scans at all declinations. The standard deviation was calculated for a right ascension scan at each declination. The spectrum deviates from the Gaussian distribution in the lower and upper regions beyond $|3\sigma|$. These deviations may possibly be able to be understood as a result of using overlapping windows. The direction of the maximum excess is $(\alpha, \delta) = (1^h 1' 30'', -61.0^\circ)$ with 4.7σ . The directions with excesses $\geq 3\sigma$ and $\geq 4\sigma$ are shown in Fig. 22 by dots and boxes, respectively. We looked for nearby, active objects to these excess points in the x-ray catalogue, and found no active objects within a 3° opening angle from those directions with excesses $\geq 3.5\sigma$. In Table II we list the right ascensions and declinations of the directions with excesses $\geq 4\sigma$.

A similar search of the southern sky was made by the SPASE group [43] using data collected between April and September 1988. They reported a 4.5σ excess at $(\alpha, \delta) = (174.5^\circ, -62.5^\circ)$. A search of our total database from October 1987 to January 1992 yielded no significant excess in this direction.

VIII. SUMMARY AND DISCUSSION

We have described the JANZOS experiment in some detail, and, in particular, the array of scintillators which

is used for observations at ultrahigh energies. The experiment was planned primarily to monitor UHE and VHE γ -ray emission from supernova 1987A, and to study the acceleration of cosmic rays by the neutron star which may have been born in the supernova. The array operated for 1229.16 days out of 1568 calendar days (duty cycle 78.4 %) between October 1987 and January 1992. About 80 million air shower events were recorded in that time.

The array is able to determine the arrival direction of cosmic rays with energies ~ 100 TeV within an error of $\sim 1^\circ$. This has been confirmed experimentally by comparison measurements made with the JANZOS array of Čerenkov mirrors, and by the shadowing effect of cosmic rays by the Sun and Moon. The operation of the array between October 1987 and January 1992 was quite stable, and the database of arrival directions is nearly isotropic in the direction of changing right ascension. As a consequence of this, point sources of γ rays may be searched for by scanning the database for peaks.

We studied SN 1987A throughout the period October 1987 to January 1992. During this time no continuous emission of UHE γ rays was detected. Also, the monthly variation was consistent with Poissonian fluctuations of the background. We obtained an upper limit on the average flux above 190 TeV of $1.0 \times 10^{-13} \text{cm}^{-2} \text{s}^{-1}$ at the 95% confidence level.

The activity of the neutron star in SN 1987A is not confirmed yet in the optical [2], radio [3] region, or UHE γ -ray regions. It is expected that a collision between ejecta from the supernova and circumstellar matter will commence soon [44]. In this collision some fraction of the kinetic energy of the ejecta ($\sim 10^{51}$ erg) may be converted to high energy cosmic rays. The shock wave produced by the collision may accelerate charged particles up to an energy of ~ 1000 TeV. We can expect γ rays with energies of ~ 100 TeV to be produced as a result of this particle acceleration. This mechanism is similar to the one proposed [9] to explain the TeV γ -ray flare observed on 14–15 January 1988 [5]. Although this collision is expected to continue for more than a few decades, the expected γ -ray flux is small, because the density of matter in the acceleration region is expected to be low. An improvement in the sensitivity of current detection

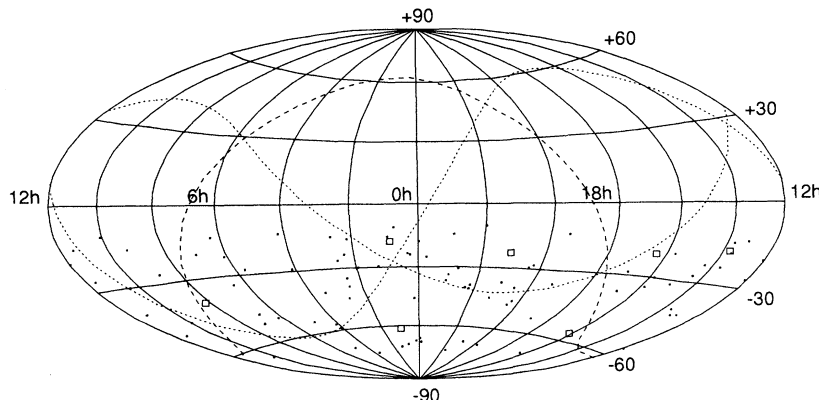


FIG. 22. Excess directions scan for $-10^\circ \geq \delta \geq -75^\circ$. The dots show the excess directions with $\sigma > 3.0$ and solid boxes show them with $\sigma > 4.0$. The dashed line is the equator and the dotted lines are meridians of $0^\circ, 90^\circ, 180^\circ,$ and 270° in the Galactic coordinate system.

techniques may be required to detect this type of emission.

We monitored several objects other than SN 1897A. In particular we monitored Vela Pulsar, Vela X-1, LMC X-4, Sco X-1, Cen X-3, SMC X-1, Galactics Center, Cen A, 4U1145-619, 2A1822-371, and PSR1706-44 at energies $\sim 10^{14}$ eV. Steady emission was not observed from any of these objects. We obtained upper limits on the fluxes as given in Table I. A comparison of our results with those obtained in other experiments is shown in Figs. 14–20. For some of these other objects, episodic or pulsed emission at energies $\gtrsim 10^{15}$ eV has been reported by other groups. We shall search out database for such emission in the future.

We searched our database for evidence of UHE γ emission by unknown objects in the southern sky. The maximum excesses were found at the positions listed in Table II. None of these positions corresponds to a known, active object, and further observations are required to determine if they correspond to unknown astronomical objects, or if the excesses are just statistical fluctuations of the database.

We studied the electron size spectrum of air showers for the purpose of calibrating the array and checking our Monte Carlo studies. For the observation of charged cosmic rays, the JANZOS scintillator array covers an interesting region (100–3000 TeV). This energy range is just below the well-known kink in the cosmic-ray energy spectrum called the “knee” (~ 5000 TeV). Some authors have proposed that cosmic rays with energies above the knee are produced by different sources from those below the knee [45]. Although there are measurements of the energy spectrum of cosmic rays by air shower experiments around and above the energy of the knee [10,46], measurements of the cosmic ray spectrum at 100–3000 TeV are rather sparse [11]. In the future we plan to increase the dynamic range of the detector by a factor of 10, enabling measurements to be made from 100 TeV up to 30 000 TeV. This energy range covers both the lower and upper regions of the “knee.”

The raw arrival distribution of cosmic rays recorded by the array was examined to study the systematic effects which may be in the experiment. The uniformity of the distribution was found to be comparable, without correcting for pressure and temperature variations, with that obtained in studies specifically aimed at the anisotropy of the arrival distribution. The effects of pressure and temperature variations will be included in future analyses to enable the anisotropy of the cosmic ray arrival distribution to be measured at ultrahigh energies. If a change in the source of cosmic rays occurs near the “knee,” it may be reflected in an anisotropy of arrival directions, as well as in the energy spectrum. Thus a detector which covers this energy region may make useful observations of both the energy spectrum and the arrival direction anisotropy of cosmic rays.

ACKNOWLEDGMENTS

We are grateful to Professor J. Arafune, Professor G. Austin, Professor B. Davis, and Professor H. Sugawara for their support. We acknowledge Dr. D. Robinson for his hospitality at Black Birch site. We appreciate the cooperation of the New Zealand Ministry of Works and Development (Blenheim branch). This work was supported in part by Grants-in-Aid for Scientific Research from the Ministry of Education, Science and Culture, the Yamada Foundation, the Inoue Foundation, the Japan-New-Zealand Foundation, the University of Auckland Research Committee, the University of Auckland Finance Committee, The New Zealand Scientific Research Distribution Committee, the New Zealand University Grants Committee, the Australian Department of Industry, Technology, and Commerce, and the Donovan Foundation. A part of analysis was carried out by the FACOM M780 in the computer room of the Institute for Nuclear Study, University of Tokyo.

-
- [1] H. Sato, *Prog. Theor. Phys.* **58**, 549 (1977); V.S. Berezinsky and O.F. Prilutsky, *Astron. Astrophys.* **66**, 325 (1978); M.M. Shapiro and R. Silberberg, in *Relativity, Quanta and Cosmology*, edited by F. DeFinis (Johnston Reprint Corporation, New York, 1979), Vol. 2, p. 745; T.K. Gaisser, A. Harding, and T. Stanev, *Nature (London)* **329**, 314 (1987); V.S. Berezinsky and V.L. Ginzburg, *ibid.* **329**, 807 (1987); Y. Yamada *et al.*, *Prog. Theor. Phys.* **79**, 416 (1988); T.K. Gaisser, A. Harding, and T. Stanev, *Astrophys. J.* **345**, 423 (1989).
- [2] N.B. Suntzeff, M.M. Phillips, D.L. Depoy, J.H. Elias, and A. Alkser, *Astron. J.* **102**, 1118 (1991); P. Bouchet, I.J. Danziger, and L.B. Lucy, *ibid.* **102**, 1135 (1991).
- [3] L. Staveley-Smith *et al.*, *Nature (London)* **355**, 147 (1992).
- [4] I.A. Bond *et al.*, *Phys. Rev. Lett.* **60**, 1110 (1988); T.K. Gaisser *et al.*, *ibid.* **62**, 1425 (1989); T.K. Gaisser *et al.*, in *Proceedings of the Twenty First International Cosmic Ray Conference*, Adelaide, Australia, 1990, edited by R.J. Protheroe (Australia Graphic Service, Northfield, South Australia, 1990), Vol. 2, p. 209; T. Kaneko *et al.*, *ibid.*, Vol. 2, p. 205; M. Finnemore *et al.*, in *Proceedings of the Twenty Second International Cosmic Ray Conference*, Dublin, Ireland, 1991, edited by M. Cawley *et al.* (Reprint Ltd., Dublin, Ireland, 1991), Vol. 2, p. 388.
- [5] I.A. Bond *et al.*, *Phys. Rev. Lett.* **61**, 2292 (1988).
- [6] I.A. Bond *et al.*, *Astrophys. J.* **344**, L17 (1989).
- [7] I.A. Bond *et al.*, in *Proceedings of the Twenty First International Cosmic Ray Conference* [4], Vol. 2, p. 198; I.A. Bond *et al.*, *ibid.*, Vol. 2, p. 210.
- [8] W.H. Allen *et al.*, in *Proceedings of the Twenty Second International Cosmic Ray Conference* [4], Vol. 1, p. 376; W.H. Allen *et al.*, *ibid.*, Vol. 1, p. 368; H. Yoshii *et al.*, *ibid.*, Vol. 1, p. 364.
- [9] M. Honda, H. Sato, and T. Terasawa, *Prog. Theor.*

- Phys. Lett. **82**, 315 (1989); S. Hayakawa, in *Fifth Marcel Grossmann Meeting*, Proceedings, Perth, Australia, 1988, edited by D. Blair and M. Buckingham (World Scientific, Singapore, 1989).
- [10] M. Nagano *et al.*, J. Phys. G **10**, 1295 (1984).
- [11] N.L. Grigorov *et al.*, in *Proceedings of the Twelfth International Cosmic Ray Conference*, Hobart, Australia, 1971, edited by A.G. Fenton and K.B. Fenton (University of Tasmania, Hobart, Tasmania, Australia, 1971), Vol. 5, p. 1746.
- [12] M. Ryan, J.F. Ormes, and V.K. Balasubrahmanyam, Phys. Rev. Lett. **28**, 985 (1972).
- [13] R.W. Clay, P.R. Gerhardy, and D.F. Liebing, Aust. J. Phys. **37**, 91 (1984); D.J. Bird and R.W. Clay, Proc. Astron. Soc. Austr. **8**, 226 (1990).
- [14] R.J. Protheroe, R.W. Clay, and P.R. Gerhardy, Astrophys. J. **280**, L47 (1984); R.J. Protheroe and R.W. Clay, Nature (London) **315**, 205 (1985); R. Meyhandan, B.R. Dawson, R.J. Clay, L. Horton, J. Ulrichs, and M.M. Winn, Astrophys. J. **391**, 236 (1992).
- [15] Meyhandan *et al.* [14].
- [16] D. Ciampa, R.W. Clay, and P.G. Edwards, Astrophys. J. **346**, 151 (1989).
- [17] R.W. Clay, R. Meyhandan, L. Horton, J. Ulrich, and M.M. Winn, Astron. Astrophys. **255**, 167 (1992).
- [18] S.C. Tonwar, N.V. Gopalakrishnan, S.K. Gupta, M.R. Rajee, B.V. Sreekantan, and R. Srivastan, Phys. Rev. Lett. **67**, 2248 (1991).
- [19] R. Meyhandan, R.W. Clay, B.R. Dawson, and P.G. Edwards, J. Phys. G **19**, L1 (1993).
- [20] J. Poirier and S. Mikocki, Nucl. Instrum. Methods **A257**, 473 (1987); S.D. Bloomer, J. Linsley, and A.A. Watson, J. Phys. G **14**, 645 (1988).
- [21] T.K. Gaisser *et al.*, in *Proceedings of the Twenty Second International Cosmic Ray Conference* [4], Vol. 1, p. 516.
- [22] S. Mikocki *et al.*, J. Phys. G **13**, L85 (1987); P.J.V. Eames *et al.*, in *Proceedings of the Twentieth International Cosmic Ray Conference*, Moscow, USSR, 1987, edited by V.A. Kozyarivsky *et al.* (Nauka, Moscow, 1987), Vol. 2, p. 449; A.M. Hillas, *ibid.*, Vol. 6, p. 432; B. Dingus, Ph.D. thesis, University of Maryland, 1988; P.G. Edwards, T. Kifune, and M. Mori, Proc. Astron. Soc. Austr. **8**, 161 (1989); M. Amenomori *et al.*, Nucl. Instrum. Methods **A288**, 619 (1990).
- [23] W.H. Allen *et al.*, Astrophys. J. **405**, 554 (1993).
- [24] K. Kasahara and S. Torii, Comput. Phys. Commun. **64**, 109 (1991); K. Kasahara, S. Torii, and T. Yuda, in *Proceedings of the Sixteenth International Cosmic Ray Conference*, Kyoto, Japan, 1979, edited by S. Miyake (University of Tokyo, Tokyo, Japan, 1979), Vol. 13, p. 70.
- [25] J. Linsley, in *Proceedings of the Eighteenth International Cosmic Ray Conference*, Bangalore, India, 1983, edited by N. Durgaprasad *et al.* (Indian National Scientific Documentation Centre, New Delhi, India, 1983), Vol. 12, p. 135.
- [26] R.J. Protheroe, Astron. Expr. **1**, 33 (1984).
- [27] P.M. Chadwick *et al.*, Astrophys. J. **333**, L19 (1988).
- [28] B.C. Raubenheimer *et al.*, Astrophys. J. **293**, L11 (1988).
- [29] M. Finnemore *et al.* [4].
- [30] D. Ciampa *et al.*, Astrophys. J. **326**, L9 (1988).
- [31] I.A. Bond *et al.* [4].
- [32] W.H. Allen *et al.*, Astrophys. J. **403**, 239 (1993).
- [33] C.C.G. Bowden, S.M. Bradbury, P.M. Chadwick, J.E. Diekinsen, N.A. Dipper, P.J. Edwards, E.N. Lindon, T.J.L. McComb, K.J. Orford, S.M. Rayner, and K.E. Turver, J. Phys. G **18**, L127 (1992).
- [34] G.J. Thornton, P.G. Edwards, A.G. Gregory, J.R. Patterson, M.D. Roberts, E.P. Rowell, and N.I. Smith, in *Proceedings of the Twenty Second International Cosmic Ray Conference* [4], Vol. 1, p. 336.
- [35] A.R. North, B.C. Raubenheimer, O.C. de Jager, A.J. van Tonder, and G van Urk, Nature (London) **326**, 567 (1987).
- [36] B.C. Raubenheimer, A.R. North, O.C. de Jager, and H.I. Nel, Astrophys. J. **336**, 394 (1989).
- [37] W.W. Clay *et al.*, in *Proceedings of the Twentieth International Cosmic Ray Conference* [22], Vol. 1, p. 250.
- [38] K. Suga *et al.*, in *Proceedings of the Nineteenth International Cosmic Ray Conference*, La Jolla, California, 1985, edited by F.C. Jones, J. Adams, and G.M. Mason, NASA Conf. Publ. 2376 (Goddard Space Flight Center, Greenbelt, MD, 1985), Vol. 1, p. 277.
- [39] K.T.S. Brazier, A. Carraminana, P.M. Chadwick, N.A. Dopper, E.W. Lindon, V.G. Mannings, T.J.L. McComb, K.J. Orford, S.M. Ragner, K.E. Turver, and D.C. Willam, in *Proceedings of the Twenty First International Cosmic Ray Conference* [4], Vol. 2, p. 296.
- [40] A.R. North, C. Brink, K.S. Cheng, O.C. deJager, H.I. Nel, and B.C. Raubenheimer, in *Proceedings of the Twenty First International Cosmic Ray Conference* [4], Vol. 2, p. 275.
- [41] J.E. Grindlay *et al.*, Astrophys. J. **197**, L9 (1975).
- [42] A. Carraminana *et al.*, Astron. Astrophys. **228**, 327 (1990).
- [43] D.J. Fegan, in *Proceedings of the Twenty First International Cosmic Ray Conference* [4], Vol. 11, p. 23.
- [44] E.J. Wampler *et al.*, Astrophys. J. **362**, L13 (1990); P. Jackson *et al.*, *ibid.* **369**, L63 (1991).
- [45] G. Auriemma *et al.*, in *Proceedings of the Twenty Second International Cosmic Ray Conference* [4], Vol. 2, p. 101; J. Wdowczyk and A.W. Wolfendale, Annu. Rev. Nucl. Part. Sci. **39**, 43 (1989), and the references therein.
- [46] T.V. Danilova *et al.*, in *Proceedings of the Fifteenth International Cosmic Ray Conference*, Plovdiv, Bulgaria, 1977 (Bulgarian Academy of Science, Plovdiv, 1977), Vol. 8, p. 129; F. Kakimoto *et al.*, in *Proceedings of the Seventeenth International Cosmic Ray Conference*, Paris, 1981 (Centre d'Etudes Nucléaires de Saclay, Gif-sur-Yvette, France, 1981), Vol. 11, p. 254.